

13-Defects, Microstructures and Textures

We will discuss these techniques, showing their possibilities and limitations. For instance we will show how it is possible to correct a varying background which often exists in the topographs, due to extended strains, and which severely prevents from observing small defects in the black areas of the image or enhance the visibility of an anisotropic feature. It is also possible to study an anisotropic texture in the images. Fourier and entropy techniques are complementary. We will compare their results and try to build a strategy for image analysis.

Two kinds of treatments may be considered. On-line analysis for standard features such as background correction, off-line treatment to extract special features. The scientist, having the knowledge of the contents of a topograph, is the only person able to choose between the various means of analysis. Thus a full investigation of a given topograph is a long process which must be applied to selected images only after a first rapid analysis.

PS-13.02.19 BRAGG-CASE IMAGES OF STACKING FAULTS.

By Wojciech Wierzchowski, Institute of Electronic Materials Technology, Wólczynska 133, 01-919 Warsaw, Poland and Moreton Moore*, Department of Physics, Royal Holloway, University of London, Egham, Surrey TW20 0EX, England.

Bragg-case synchrotron double-crystal images of stacking faults have been studied in a synthetic diamond. The topographs taken on the tails of the rocking curve showed well pronounced interference fringes arising from the stacking faults: the first such observation in Bragg diffraction geometry. The fringes were strongly dependent upon the angular setting, being invisible at the rocking curve maximum but gaining in contrast and becoming more closely spaced further from the maximum. These experimental images were compared with predictions of plane-wave dynamical theory and a reasonably good correspondence was obtained when the finite beam divergence was taken into account. It was found that the theoretical fringe sequences depended upon the type of stacking fault, and confirmed that the stacking faults observed were of intrinsic type.

PS-13.02.20 DOMAIN WALLS IN FERROELECTRICS. By M. Takagi* and S. Suzuki. 1-10-6, Tsurumaki, Setagaya, Tokyo. Sanyo Tsukuba RC, Tsukuba, Japan.

Images of imperfections which arise from the dynamical diffraction effect are observed on X-ray topographs of perfect or nearly perfect crystals. If a mosaic spread of a specimen crystal is a few minute of arc (which is ten times as large as that of perfect crystals), intensity in a Lang section topograph is uniform and the intensity is proportional to the integrated intensity of the Bragg reflection. Images of antiparallel domain walls and of the regions in the intermediate states of polarization reversal have been observed on the section topographs of ferroelectric NaNO_2 and thiourea crystals with such a mosaic spread. Structure of domain walls and of the intermediate state regions have been determined from dependence of the contrast of the images on the indices of Bragg reflection hkl . Studies of domain walls for NaNO_2 and thiourea, and of the intermediate state for NaNO_2 have already been reported and additional studies have been made on the polarization reversal of thiourea and on change in images of domain walls of NaNO_2 near the Curie temperature T_c . Results of these series of studies have made clear the structures of 180° domain walls and the polarization reversal procedure.

Atomic positions in positive domain and those in negative domain shift relatively. For a perovskite-type crystal such as BaTiO_3 , the relative shifts are as small as the amplitudes of thermal vibration, so that the two opposite domains are expected to be connected smoothly at an antiparallel domain boundary without any special layer. For some ferroelectrics such as NaNO_2 and thiourea the amount of the relative shift is as large as $0.5 \sim 1 \text{ \AA}$. For such ferroelectric crystals, thick 180° domain walls which connect the two opposite domains without lattice strain are expected. The structures of domain walls determined are as have been expected. Fig.1(a) is the c-projection of the unit

cell of NaNO_2 and (b) is that of domain walls where NO_2 radicals are rotated by about 50° or 130° around the c-axis from the original orientation. Fig.2 is the projection of the unit cell of ferroelectric thiourea, where full circles and the dotted circles represent the atomic positions in the positive and the negative domains respectively. The domain wall structure of thiourea determined is a modulated superstructure with long periods along the c-axis. In the structure, direction of thiourea molecules gradually varies along the c-axis between the two directions shown in Fig.2. 180° domain walls of NaNO_2 and thiourea are about $1 \mu\text{m}$ thick and in the domain wall structure atoms and molecules are at the halfway positions between the two opposite domains. On application of d. c. electric fields to NaNO_2 and thiourea, polarization reversal takes place via intermediate states. Structure of the intermediate state resembles the structure of domain wall.

The structure of domain walls of thiourea resembles that of the higher temperature phase above T_c , and topographic observation on NaNO_2 at T_c suggests the same correlation for NaNO_2 . These structural correlations would be applied for any ferroelectric for which the atomic shift between the two opposite domains is far larger than the amplitudes of thermal vibration.

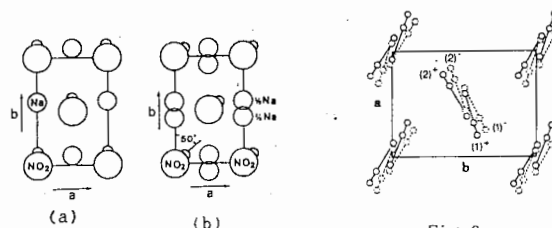


Fig.1

Fig.2

PS-13.02.21 STRUCTURE FACTORS OF LAYER SYSTEMS - EXAMPLE: BRAGG REFLECTORS (GaAs/AlAs)/GaAs.

By R. Koehler* and B. Jenichen**, *MPG-AG Roentgenbeugung, Berlin, **Paul-Drude-Institut, Berlin, Germany.

Shifts of the atomic positions inside a layers system have a strong influence on the diffracted intensities even for high order satellites and, hence, have to be described correctly. At these high orders the Fourier components of the term $\exp(-ihu)$ (h : diffraction vector; u : shift in the atomic positions as compared to a reference lattice) might be negligible but neighboring high Fourier orders of the electric susceptibility $\chi_h(r)$ are combined with low orders of the exponential. For that reason the concentration profile inside a layer stack of a quasi binary compound cannot be calculated straightforward from the diffraction curve.

On the other hand due to intermixing of Fourier orders the structure factors also depend on the phases of the Fourier components. If the satellite reflections are well separated a simulation procedure based on the integrated intensities of the satellites and on the Fourier transform of the mo-

13-Defects, Microstructures and Textures

365

del of the layer structure is feasible. For nearly periodic systems the procedure is simple enough to be performed automatically. This is demonstrated for several Bragg reflectors on 001 oriented GaAs substrates. Satellites up to more than the 20th order are well fitted by the automatic procedure.

PS-13.02.22 THE BRAGG-CASE DIFFRACTION PATTERNS OF ION-IMPLANTED LAYERS. By K. Wieteska¹⁾, W.K. Wierzchowski²⁾ and J.K. Maurin¹⁾, ^{1)Institute of Atomic Energy, Świerk-Otwock,} ^{2)Institute of Electronic Materials Technology, Warsaw, Poland.}

4-5 MeV α -particles implanted layer in silicon were studied using double-crystal method. In actual case most of the implanted ions is expected to be concentrated in a thin layer situated at the depth of several microns under the surface. The rocking curves of the layers exhibited distinct subsidiary maxima and the topographs contained systems of fringes.

In order to explain the results we discussed theoretical diffraction patterns obtained both with plane-wave approximation and by numerical integration of Takagi equations. In the last case we took into account the continuous distribution of the ions and related strains. In both cases we studied the influence of different phase shift introduced by the destroyed layer.

On the base of theoretical models we proved that the fringe systems observed in the topographs are due to the variation of the thickness of the destroyed layer, while the formation of the subsidiary maxima in the curves is connected with the thickness of the shot-through layer. The destroyed layer introduce additional phase factor multiplying the whole system of subsidiary maxima with reciprocal phases on the two sides of the rocking curve.

The important feature of the experimental rocking curves consisting in the location of the most maxima on low angle side and the increase of their period with lower angles was obtained assuming the strain gradient in the shot-through layer. It may be expected that the strain gradient causes the curvature of the trajectories and subsequent diminishing of the subsidiary maxima period. This effect should be stronger close to the main peak.

PS-13.02.23 STROBOSCOPIC OPTICAL IMAGING OF SURFACE ACOUSTIC WAVES. By W. Graeff^{*}, HASYLAB at DESY, Hamburg, Germany and K. Wieteska, Institute of Atomic Energy, Świerk-Otwock, Poland.

Surface acoustic waves (SAW) were already investigated by X-ray stroboscopic topography using synchrotron radiation from the storage ring. The dominating origin of the contrast observed in stroboscopic SAW topography is the focusing of reflected X-rays by traveling acoustic wave troughs and defocusing by wave crest, thus forming the orientation contrast. The contrast was studied by ray tracing calculations with approximating the Bragg reflection by a simple mirror reflection from a corrugated surface (Cerva & Graeff, phys. st. sol. (a) **82**, 35 (1984)). However, this model is not restricted to X-ray reflection, but holds for visible light as well. The visible part of synchrotron radiation from DORIS was used to illuminate a LiNbO₃ crystal surface. Surface acoustic waves were excited at 35.4 MHz with 10 V applied to an interdigital transducer deposited on the crystal surface. With the Rayleigh wavelength $\Lambda = 100 \mu\text{m}$ and wave amplitude $a_s = 0.9 \text{ nm}$, the focal distance was $D_F \approx 10 \text{ cm}$. The image was observed by two ways; either using the lunette and then putting the real image created behind the eyepiece into the microscope to take the picture or directly applying a simple microscope above the sample with the possibility to shift it up and down, to coincide the focal point

of the corrugated surface of the sample and the focal point of the objective of the microscope. The pictures were taken using the lunette-microscope combination. In principle, the simplest and the most elegant way to take the picture would be to put the camera without any optical system directly on the path of the reflected beam at the focal plane of waved crystal surface. Using the microscope adjusted above the sample it was possible to observe two real images created at the distances 10 and 20 cm corresponding to the D_F and $2D_F$ and one virtual image at the distance of D_F below the surface.

PS-13.02.24 SYNCHROTRON X-RAY TOPOGRAPHY STUDIES OF TWINNING IN NdP₅O₁₄ SINGLE CRYSTALS. By X.R. Huang^{*}, Z.W. Hu, and S.B. Jiang, National Laboratory of Solid State Microstructures, Nanjing University, P.R. China

An investigation of twin structures of NdP₅O₁₄ (NPP) single crystals in monoclinic phase has been undertaken using white-beam synchrotron X-ray topography. The so called a-type domain walls along a-axis related to the (001) twin plane are clearly present in the topographs. The angular shifts that arise from the twins are directly measured using different diffraction topographs taken with different diffraction vectors. From the shifts in the topographs, the twin and matrix regions in the NPP crystal can be easily distinguished. With the measurements of shifts in different topographs, the monoclinic distortion angle δ ($\delta = \beta - 90^\circ$) is calculated which is in good agreement with the unit cell parameters. On the other hand, from the parameters and the twinning configurations of NPP, we have simulated the Laue patterns which are well consistent with the experimental results. With these results, the twin structure in NPP is discussed. The changes of angular shifts with a small shear force applied along the [001] direction are revealed and discussed.

PS-13.02.25 SYNCHROTRON RADIATION TOPOGRAPHY STUDIES OF PLANAR DEFECTS IN POTASSIUM NIOBATE TANTALATE. By P.Q. Huang^{*}, J.Q. Zhu^{*}, Z.W. Hu, S.B. Jiang, and D. Feng, National Laboratory of Solid State Microstructures and Physics Department, Nanjing University, China, *Shanghai Institute of Building Materials, Shanghai 200434, China

The Fe-doped flux-grown KTa_{1-x}Nb_xO₃ (KTN) with composition on the margin of the cubic phase zone has been studied by white-beam synchrotron X-ray topography. It is shown that growth bands in flux-grown KTN are primary planar defects which lie along the [010] growth direction. A set of [100] oriented planar defects in contrast is revealed by tuning the synchrotron radiation, and the contrast reversal of the planar defects is displayed in antiparallel reflections. The intense anomaly in contrast is interpreted in terms of anomalous scattering associated with antiparallel domains. The origins of the dominant formation of the 180°C domains are discussed.